DYNAMIC INELASTIC STRUCTURAL RESPONSE ASSOCIATED WITH LARGE SODIUM-WATER REACTIONS IN LMFBR HEAT TRANSPORT SYSTEMS

R.A. VALENTIN, H.-C. LIN, B.-J. HSIEH

Components Technology Division,
Argonne National Laboratory, Argonne, Illinois 60439, U.S.A.

SUMMARY

Failure of a steam tube in a Liquid Metal Fast Breeder Reactor (LMFBR) evaporator or superheater results in a large exothermic sodium/water reaction and generates pressure pulses far in excess of nominal operating pressures. To determine the structural integrity of the heat transport system and to model the transient behavior of the reaction products relief system, it is necessary to predict the inelastic response of several components. This paper develops models for the dynamic plastic response of the shell structures within the system and also the dynamic plastic response of the relief system rupture discs. These two problems require completely different mathematical formulations for efficient solution. A comparison between the two methods is included as well as their relationship to the comprehensive analysis system being developed for treating the entire sodium/water reaction event.

A primary consideration in developing dynamic inelastic solutions for both the steam generator shell and rupture discs is that, in their final form, they can be specialized to only those problems of interest and integrated into a comprehensive code without requiring extensive computational time or excessive core storage. For the shell problems, the method chosen is based on the recently developed endochronic theory of viscoplasticity. This allows a problem formulation that can treat essentially arbitrary material property descriptions, include strain-rate dependence, and not require the definition of a yield surface. The model developed is the first application of this theory to the dynamic behavior of thin shells and uses a method-of-characteristics solution of the governing equations. This solution exhibits both the required numerical stability and the needed machine efficiency. Determination of the dynamic response of rupture discs, while somewhat similar in requiring the option of plastic material behavior, differs in that it is essentially a small strain, large displacement phenomena. This has been modeled through the use of a recently developed convected coordinate finite element method. The resulting code has been used to explore the initial buckling of rupture discs and relate this to their static failure characteristics.

The results obtained illustrate dynamic plastic wave propagation in a steam generator shell and final deformations resulting from typical pressure pulses generated by large sodium/water reactions. For similar pressure loadings, the early dynamic behavior of typical secondary system rupture discs is illustrated in a series of parametric studies. Since both methods are capable of treating certain special problems not involving large displacements, a sample problem of this type is included. Due to the lack of experimental data in the area of dynamic plasticity, such intercomparisons are a basic tool in code validation and are useful in examining numerical stability and relative accuracy of the methods. A short discussion is included on the relationship of these predictions of structure response to the on-going development of the comprehensive sodium/water reaction code SWAAM-I.

1. Introduction

The pressures generated by a large sodium/water reaction in an LMFBR steam generator are sufficiently high that several regions on the sodium side of the unit and in the intermediate heat transport system can experience inelastic deformation. The system piping and intermediate heat exchangers, while subjected to transients above their nominal design pressures, are unlikely to undergo plastic deformation due to design margins, the various attenuation mechanisms acting near the reaction zone, and the operation of the reaction product relief system. There are, however, two areas where inelastic response must be considered -- the steam generator flow shroud and the rupture disk assembly that activates the relief system. For specific classes of large water leaks, there are certainly other areas where large dynamic structural loads are an important factor; however, the two cases mentioned are currently involved in design basis calculations and deserve special consideration.

The dynamic response of the flow shroud is of importance not because of damage done to the shroud but because various flow baffles that support the tube bundle are connected to the shroud. Any appreciable deformation of the shroud can result in large rotations of the baffles and, from the resultant loading of the tubes, could cause additional failures which would increase the severity of the sodium/water reaction. It is also true that the shroud acts as protection for the steam generator shell and that an accurate knowledge of its response and the coupling of this to the outer shell may allow one to demonstrate that the main shell is acceptable for requalification even after a large disruptive event.

The case of the rupture disk response is somewhat different. One is now talking of a structure that must fail under a given class of dynamic loads. Further, in designs of the type that are common in US plants such as the Clinch River Breeder Reactor (CRBR), the disk assembly is located as close as possible to the unit to insure a rapid opening of the relief system and to thereby minimize the duration of local overpressures. In designs of this type, a variation of a few milliseconds in the time required to activate the relief system can significantly alter the damage potential of the event. For this reason, an accurate measure of dynamic disk response is needed and, if possible, a criteria defining "dynamic rupture pressure". To provide such information it is necessary to study not small strain inelastic response of the type experienced by the flow shroud but to be able to treat large displacement, small-strain inelastic effects.

Since the modular nature of the comprehensive code (SWAAM-I) being developed by ANL to study large sodium/water reactions makes it relatively easy to introduce a specialized method to analyze a single component not closely coupled to the reaction region, it is possible to use different methods for the shell response and for the rupture disk. In particular, since the rupture disk is physically isolated from much of the system and acts only for a relatively short duration during the transient, it is desirable to provide a specific routine that incorporates its unique features (large displacements of a fixed geometry structure) rather than having this special capability built into the more general shell routine.

The design oriented requirements of SWAAM-I place a premium on having individual code modules that are flexible, compact, and not overly demanding of core space or running time. This poses a special problem for the structural response calculations since they must consider plasticity effects and, hence, are inherently nonlinear. A particular difficulty associated with plastic response involves the extensive bookkeeping necessary to trace the evolution of the yield surface and the position of the stress state of every point with respect to this surface. In the shell analysis module, this difficulty has been partially overcome by employing a relatively recent formulation for the viscoplastic response of materials termed endochronic theory [1]. In this formulation, it is not necessary to define a yield surface and the resulting shell equations form a quasi-linear hyperbolic system. A solution can then be obtained by the method of characteristics and, hence, the problem of fluid/shell interaction is more tractable since a characteristic solution is also used for the two-dimensional hydrodynamics [2].

The rupture disk dynamics is treated in terms of conventional plasticity theory and a recently developed convected coordinate finite-element method which allows large-displacements while being limited to small-strains [3]. It is possible to follow the details of the disk displacement as a function of an arbitrary pressure history which, together with a suitable design-dependent definition of the displacement required to open the disk, provides information on the initiation of flow into the relief piping and the pressure-relief feedback to the sodium piping.

2. Inelastic Shell Response Formulation

The fundamentals of endochronic viscoplasticity were developed by Valanis [1] and a summary of the elements of the theory as applied in the development of shell equations is found in Lin [4]. An essential factor in the theory is that the history of deformation is not expressed in terms of real clock-time but by a measure that is a time-like material property. This time measure, $d\zeta$ is in general defined in terms of a positive semi-definite fourth-order material tensor and the right Cauchy-Green deformation tensor. In the restricted case of an isotropic material with no strain-rate dependence as considered in the present formulation one has

$$d\zeta^2 = K_1\, d\varepsilon_{kk}\, d\varepsilon_{\ell\ell} + K_2\, d\varepsilon_{ij}\, d\varepsilon_{ij} \tag{1}$$

where $K_1 + K_2/3 \geq 0$, $K_2 \geq 0$, and K_1 and K_2 may not both be zero. In addition, a time scale $z(\zeta)$ is introduced such that $dz/d\zeta > 0$. For small strains and small changes in temperature with an assumed elastic hydrostatic response, the basic constitutive equations reduce to

$$s_{ij} = 2 \int_0^z \mu(z - z') \frac{\partial e_{ij}}{\partial z'}\, dz', \tag{2}$$

$$\sigma_{kk} = 3K\, \varepsilon_{kk}\,, \tag{3}$$

where s_{ij} and e_{ij} are the deviatoric stress and strain tensors, K is the bulk modulus, and $\mu(z)$ is a material heredity function. If one introduces a simplified material description,

$$\mu(z) = \mu_o \exp(-\alpha z) \quad , \quad dz = d\zeta(1+\beta\zeta)^{-1}, \tag{4}$$

where μ_o, α, and β are material constants, then Eq. (2) reduces to

$$2\mu_o \frac{d\underset{\sim}{e}}{d\zeta} = \frac{\alpha \underset{\sim}{s}}{1+\beta\zeta} + \frac{d\underset{\sim}{s}}{d\zeta} \quad . \tag{5}$$

In the restricted sense used in this paper, Eqs. (1), (3), (5) are the complete constitutive equations of the endochronic theory of plasticity.

For a long circular cylindrical shell with mean radius R and thickness H, the equations of motion in the axial direction, x, and radial direction, r, are given by:

$$\frac{\partial \sigma_x}{\partial x} + \frac{\sigma_{xr}}{R} = \rho \frac{\partial u}{\partial t} \quad , \tag{6}$$

$$\frac{\partial \sigma_{xr}}{\partial x} + \frac{p(x,t)}{H} - \frac{\sigma_\theta}{R} = \rho \frac{\partial w}{\partial t} \quad , \tag{7}$$

where ρ is the density, p is the internal pressure, u is the axial velocity, w is the radial velocity, σ_x, σ_θ are the stress components in the x and θ directions, and σ_{xr} is the only non-zero shear stress. In addition, we have the following compatibility conditions:

$$\frac{\partial \varepsilon_x}{\partial t} = \frac{\partial u}{\partial x} \quad , \qquad \frac{\partial \varepsilon_\theta}{\partial t} = \frac{w}{R} \quad , \qquad \frac{\partial \varepsilon_{xr}}{\partial t} = \frac{1}{2}\frac{\partial w}{\partial x} \tag{8}$$

From the definition of $\underset{\sim}{e}$ and $\underset{\sim}{s}$, it is possible to express the time measure approximately as

$$\beta d\zeta = \pm \beta_1 \left[1 + \left(\frac{d\varepsilon_x}{d\varepsilon_\theta}\right)^2\right]^{1/2} d\varepsilon_\theta \quad , \tag{9}$$

where $\beta_1 = E_t/\sigma_o$, E_t is the asymptotic slope of the stress-strain curve for large strain, σ_o is the intercept of this slope with the stress axis, and the positive sign holds for straining while the negative sign is for unstraining of $d\varepsilon_\theta$. Using (9) and Eqs. (1), (3), (5), and the compatability conditions (8) results in the following:

$$\left.\begin{aligned}
&\frac{\partial \sigma_x}{\partial t} + \frac{\partial \sigma_\theta}{\partial t} - d_1 \frac{\partial u}{\partial x} = d_2 \frac{w}{R} \\
&\frac{\partial \sigma_x}{\partial t} - \frac{\partial \sigma_\theta}{\partial t} - d_4 \frac{\partial u}{\partial x} = d_3 \frac{w}{R} \\
&\frac{\partial \sigma_{xr}}{\partial t} - \mu_o \frac{\partial w}{\partial x} = -a_3 \frac{w}{R}
\end{aligned}\right\} \tag{10}$$

where

$$d_1 = E_o\,(1-\nu)^{-1},\ d_2 = (E_o \mp a_1)(1-\nu)^{-1},\ d_3 = (-E_o \mp a_2)(1+\nu)^{-1},\ d_4 = E_o(1+\nu)^{-1},$$

$$a_1 = \frac{1}{2}\,\alpha'_1\,\gamma\,(\sigma_x+\sigma_\theta),\quad a_2 = \frac{3}{2}\,\alpha'_1\,\gamma\,(\sigma_x-\sigma_\theta),\quad a_3 = \alpha_1\,\gamma\,\sigma_{xr},$$

and

$$\gamma = \left[1 + \left(\frac{d\varepsilon_x}{d\varepsilon_\theta}\right)^2\right]^{1/2} (1 + \beta\zeta)^{-1}.$$

In the above, the initial slope of the uniaxial stress strain curve, E_o, and the initial Poisson's ratio, ν, are related to μ_o and K by

$$E_o = 3\mu_o\left(1 + \frac{\mu_o}{3K}\right)^{-1},\quad \nu = \frac{E_o}{2\mu_o} - 1,$$

and, in addition,

$$\alpha' = \frac{E_o}{3\mu_o}\,\alpha,\quad \alpha'_1 = \alpha'\beta_1,\quad \alpha_1 = \alpha\beta_1.$$

The wave propagation problem in the shell is thus defined by Eqs. 6, 7, and 10 together with appropriate boundary conditions. These equations together with the differential auxiliary equations may be written in matrix form as

$$[A]\ \{X\} = \{B\} \tag{11}$$

where

$$[A] = \left[\begin{array}{ccccc|ccccc}
 & & & -d_4 & & 1 & 1 & & & \\
 & & & -d_4 & & 1 & -1 & & & \\
 & & & & -\mu_o & & & 1 & & \\
1 & & & & & & & & -\rho & \\
 & & 1 & & & & & & & -\rho \\
\hline
dx & & & & & dt & & & & \\
 & dx & & & & & dt & & & \\
 & & dx & & & & & dt & & \\
 & & & dx & & & & & dt & \\
 & & & & dx & & & & & dt
\end{array}\right]$$

$$\{X\} = \left\{\frac{\partial\sigma_x}{\partial x}, \frac{\partial\sigma_\theta}{\partial x}, \frac{\partial\sigma_{xr}}{\partial x}, \frac{\partial u}{\partial x}, \frac{\partial w}{\partial x}, \frac{\partial\sigma_x}{\partial t}, \frac{\partial\sigma_\theta}{\partial t}, \frac{\partial\sigma_{xr}}{\partial t}, \frac{\partial u}{\partial t}, \frac{\partial w}{\partial t}\right\}^T,$$

and

$$\{B\} = \left\{\frac{d_2 w}{R}, \frac{d_3 w}{R}, \frac{-a_3 w}{R}, \frac{-\sigma_{xr}}{R}, \frac{\sigma_\theta}{R} - \frac{p}{H}, d\sigma_x, d\sigma_\theta, d\sigma_{xr}, du, dw\right\}^T.$$

A conventional characteristics solution results in five characteristics with two related to the longitudinal wave speed, c, and two to the shear wave speed, c_s. The solution is thus obtained from:

$$d\sigma_x = \pm\rho\,c\,du - \frac{\sigma_{xr}}{R}\,dx + \frac{1}{2}\left(\frac{E_o \mp a_1}{1-\nu} + \frac{-E_o \mp a_2}{1+\nu}\right)\frac{w}{R}\,dt \ \text{ along } \frac{dx}{dt} = \pm c = \pm\sqrt{\frac{E_o}{(1-\nu^2)\rho}}, \tag{12}$$

$$d\sigma_{xr} = \pm\rho\ c_s dw - \left(\frac{p}{H} - \frac{\sigma_\theta}{R}\right) dx - a_3 \frac{w}{R} dt \text{ along } \frac{dx}{dt} = \pm c_s = \pm\sqrt{\frac{\mu_o}{\rho}} . \tag{13}$$

$$d\sigma_\theta = d\sigma_x - \frac{E_o}{1+\nu} d\varepsilon_x - \frac{-E_o \mp a_2}{1+\nu} d\varepsilon_\theta \qquad \text{along } dx = 0. \tag{14}$$

The details of the computational methods employed are given in [4]. Since the characteristics are constant, a fixed rectangular mesh is employed. Equations (12) - (14) are expressed in simple finite-difference form and, with appropriate iteration within each time step and consideration of the required stability criterion, it is possible to construct the solution in an expeditious manner for an arbitrary input of p(x,t).

3. Shell Response Results

The computational module of SWAAM-I that was written to implement the theoretical development of the previous section can also be used as an independent unit for the solution of problems not coupled to the entire sodium/water reaction event. As an illustration, we have included calculations describing the dynamic response of a shell typical of the flow shroud of the current Atomics International steam generator for the CRBR. A central segment of this shell is 42 in. between support baffles, has a radius of 18.5 in. and a thickness of 0.5 in. The material is 2-1/4 Cr - 1 Mo at 900°F. Since the example was computed independent of the remaining parts of SWAAM-I, it was necessary to supply a pressure input function. This was generated by the hydrodynamics module described in [8]. A constant volume, centered step pressure of 2000 psi was taken as the source since this is typical of the maximums observed in large sodium/water reaction experiments during the first few milliseconds.

The resulting pressure trace at the axial mid-point of the inner surface of the shell is shown in Fig. 1. The step-like behavior as a function of time is typical of such pressures and is related to the wave transit time between the center and the various surfaces. Figure 1 also shows the resultant dynamic displacement as a function of time for the same center point of the shell. Note that, in a qualitative sense, the displacement history somewhat parallels the input pressure. The third curve on Figure 1 shows the radial velocity component and is used to compute shell/fluid interaction effects when the shell code is fully coupled to the hydrodynamics module. In Fig. 2, shell displacement profiles are shown for several times. In this problem the "ends" of the shell were assumed to be simply supported at the flow baffles since we were primarily interested in determining the maximum displacements that could be expected during a relatively severe loading condition. In this respect it is worth noting that the maximum observed displacements are very small considering the high loading. Also, as shown on Fig. 3, the strain levels, while certainly in the plastic range, are within the very conservative limits one finds in current design codes for elevated temperature service. This does not, of course, indicate that a large sodium/water reaction event has negligible effect on the integrity of the internal structure of the steam generator since we have chosen to ignore many interrelated phenomena (e.g. the high transient temperatures occurring later in the event) that determine the total damage. It is still of interest, however, to note that we are discussing relatively small plastic distortions and the possibility of reuse of a "failed" steam generator is not beyond consideration.

4. Rupture Disk Dynamics -- Formulation and Results

The dynamics of the rupture disk are treated in terms of an axisymmetrical formulation of the convected coordinate finite element method discussed in detail in [3] and [5]. The basic method uses a convected coordinate system which translates and rotates but does not deform with an element. If the strains are small, the convected coordinates can be chosen and kept orthogonal and, in terms of these coordinates, the strain-deformation displacement can be shown to be linear independent of the magnitude of element displacement.

The disk is defined as a connected system of conical shell elements obtained by rotation of rectilinear beam elements about the axis of symmetry. It then becomes possible to treat the axisymmetric problem as a modified planar problem with the added condition that rotations in the plane cause circumferental strains. If $\{u\}$ are displacements referred to a fixed reference coordinate system x_i $(i = 1,2)$ and $\{d\}$ are the nodal displacements of the element, then these are related by a shape function matrix $[\phi]$ such that $\{u\} = [\phi]\ \{d\}$. Once the rigid rotation and translation of an element are obtained, the deformation displacement is

$$\{u^{def}\} = [\phi]\ \{d^{def}\}\ , \quad \{d^{def}\} = \{d\} - \{d^{rig}\}\ , \tag{15}$$

where $\{d^{rig}\}$ is the nodal displacement due to plane rigid body motion. In the convected coordinates, $\hat{x}_i$, the deformation displacements $\{\hat{d}^{def}\}$ are obtained from (15) by an orthogonal transformation. It is then possible to obtain the planar strains in convected coordinates

$$\{\hat{\varepsilon}^p\} = [E_d^p]\{\hat{d}^{def}\} \tag{16}$$

and the circumferential strain due to the deformation and rigid body motion

$$\{\varepsilon^c\} = [E_r^c]\ \{d\} + [E_d^c]\ \{\hat{d}^{def}\}\ . \tag{17}$$

Noting that the principle of virtual work is a mathematical identity and this holds even in problems involving energy dissipation, the principle is applied to each element in the convected coordinates. The total work is taken as the sum of the external and internal work of all of the elements. The equations of motion which result are

$$[M]\ \{\ddot{D}\} = \{F^e\} - \{F^i\} \tag{18}$$

where $[M]$ is a diagonal mass matrix obtained by lumping the mass of each element at the nodes in a physically consistant manner and the equivalent nodal force vectors are obtained as

$$\{F^e\} = \sum_{k=1}^{N} [L]_k\ \{f^e\}\ , \quad \{F^i\} = \sum_{k=1}^{N}\ [L]_k\ \{f^i\}\ , \tag{19}$$

by summing the contribution from all elements connected to a node. In (19), $[L]_k$ is the connectivity matrix of element k of the N elements and

$$\{f^i\} = [T]\ \int_V\ ([E_d^p] + [E_d^c])^T\ \{\hat{\sigma}\}\ dv + \int_V\ [E_r^c]^T\ \{\hat{\sigma}\}\ dv,\ \{f^e\} = \int_S\ [\phi]^T\ \{p\}\ ds, \tag{20}$$

where $[T]$ is an orthogonal transformation matrix, $\{p\}$ is the surface traction vector, and all body forces have been neglected. The equations of motion (18) are integrated in a stepwise manner using a central difference technique.

To derive the nodal forces using eqs. (20) it is necessary to obtain the stress distribution for each element in its convected coordinates. These are obtained from the strains using the constitutive law. In problems such as the rupture disk where large displacements occur it is necessary to distinguish a stress rate which is the partial with respect to time of the stress in the x_i system and a convected stress rate where the partial with respect to time is taken on the stress relative to the $\hat{x}_i$ system. It can be shown that all well-formulated constitutive relationships for small displacement problems remain valid with a direct replacement of stress (strain) rate by convected stress (strain) rate. In studying the rupture disk, linear elastic and bilinear elastoplastic constitutive relations were employed. In the latter, von Mises' yield criterion and the Prandtl-Reuss flow rule were used.

To illustrate the basic problems associated with dynamic response of steam generator rupture disks, we will concentrate on dimensions and loadings typical of those used in the Clinch River Breeder Reactor (CRBR) reaction product relief system. The basic data is:

$2A$ = dia. of base = 17 in.	θ = half-angle of opening = 28.2°
R = dome radius = 18 in.	ρ = mass density = 7×10^{-4} slugs/in^3
h = thickness = 0.071 in.	E = Young's modulus = 2.29×10^7 psi
H = apex height = 2.133 in.	ν = Poisson's ratio = 0.30

This disc as supplied by the manufacturer has a static rupture pressure of 300 psi (the classical Timoshenko static buckling pressure, P_o, as given in [6] is P_o = 431.3 psi). The results discussed in what follows are limited to elastic calculations and do not include the coupling of the disk and the sodium during the transient. The basic problem of developing dynamic rupture criterion can be understood from this simplified case. Coupling and plastic response add additional complications that will only be mentioned. Additional results on plastic response may be found in [7].

Figure 4 shows the progressive dynamic displacement of the reference rupture disk when acted on by a step pressure increase of 0.5 P_o. The calculations assume elastic material response and were carried to a time longer than that associated with rupture. In the real disk, a knife blade arrangement cuts the disk when the center reaches the apex height. In Fig. 4, the calculation shows the disk rebounding (t = 4.0 msec) when the real disk would have been cut at t ≅ 2.5 msec. The important point is that for a step pressure of half the static buckling pressure, the disk will snap through. This is typical of all results obtained neglecting coupling between the disk and sodium. The step pressure causing failure is usually somewhere between 0.3 and 0.4 of the static value; however, a precise definition of a dynamic failure pressure does not seem feasible.

To illustrate the ambiguity inherent in defining dynamic failure, consider the displacement histories of the disk center shown in Fig. 5 for various fractions of the static buckling load, P_o. For 0.3 P_o it seems likely that the disk will continue to oscillate near some equilibrium position even if the calculation is carried on for a much larger period than 2.0 msec. Also, for 0.5 P_o is it clear the disk will fail. The difficulty comes in choosing the intermediate value associated with true failure. To get better information one should plot displacement history curves for longer times and smaller steps in P_o. Since this is not practical from computational (or economic) considerations, an alternative is to calculate displacement histories for a given time (e.g. 2 msec.) for relatively large increments of P_o and to then plot maximum displacement during that time as a function of P_o and look for a qualitative change in this function as an indication of a failure level. This has been done in Fig. 6. One notes that very large displacements occur somewhere in the range 0.4 to 0.5 P_o and, hence, within the very restrictive assumptions associated with creating this figure, it would be possible to define a "dynamic rupture pressure" in this range. It remains, however, that this curve was generated for only one type of loading, no fluid interaction, and elastic material response. Thus the possible number of parameters that must be investigated before a well defined concept of dynamic failure is formulated is very large. Some of these may be of no significance but still must be checked for all cases of interest. For example, Fig. 6 shows data from both fixed and hinged disk boundary conditions and indicates that, for this particular geometry, edge conditions are relatively unimportant in determining the load causing large displacement.

5. General Conclusions and Relationships to SWAAM-I

The two code modules described in this paper are currently being integrated into the body of SWAAM-I. Preliminary indications are that, while the shell dynamics associated with large sodium/water reactions may not produce significant inelastic deformations, exact computations will require careful consideration of the interaction of the static sodium volume between the shroud and the steam generator shell. Also, for tube failures occurring near the flow windows in the shroud, there is a possible path for transmission of a larger fraction of energy into the intermediate system piping then in the central break cases consider as examples. In general, the major factors in reducing the severity of most of the sodium/water events is the geometrical attentuation associated with the large diameters of the units rather than any energy partitioning related to structural deformation.

The significance of the dynamic response of the relief system is also unresolved at this moment. Delays in opening of the disks and their location relative to the assumed break site are reflected in the pressures experienced by the Intermediate Heat Exchangers (IHX). Cases where one millisecond delays in rupture disk opening cause an increase in IHX pressure of about 25 psi are typical. It may prove more important to understand the dynamics of the rupture disk system in cases where it is necessary to assure that the system does not operate. For example, it must be demonstrated that normal secondary system transients (i.e. pump trips) do not cause disk instability that results in inadvertant dumping of the secondary sodium inventory.

References

[1] Valanis, K. C., "A Theory of Viscoplasticity Without a Yield Surface, Part I: General Theory, Part II: Applications to Mechanical Behavior of Metals," Archiwum Mechaniki Stosowanej, 23, 517-551, 1971.

[2] Shin, Y. W. and R. A. Valentin, "Two-Dimensional Fluid-Hammer Analysis by the Method of Characteristics in a Closed Axisymmetric Cylindrical Domain", Argonne National Laboratory Report ANL-8090, August 1974.

[3] Hsieh, B. J., "Nonlinear Transient Finite Element Analysis with Convected Coordinates", Ph.D. Thesis, Department of Materials Engineering, University of Illinois at Chicago Circle, June 1974.

[4] Lin, H. C., "Plastic Wave Propogation in an Axially Symmetric Circular Cylindrical Shell", Argonne National Laboratory, Components Technology Division Technical Memorandum, ANL-CT-75-27, February 1975.

[5] Belyschko, T., J. J. Kennedy and B. J. Hsieh, "Convected Coordinates for Transient Nonlinear Finite-Element Analysis", Paper M3/9, 2nd SMiRT, Berlin, Sept. 1973.

[6] Timoshenko, S., and S. Woinowsky-Krieger, Theory of Plates and Shells, McGraw-Hill, New York, 1959.

[7] Hsieh, B. J., "Dynamic Transient Analysis of Rupture Disks by the Finite Element Method", Argonne National Laboratory, Components Technology Division Technical Memorandum, ANL-CT-75-33, February, 1975.

[8] Shin, Y. W. and R. A. Valentin, "Dynamic Structural Loads Produced by Large Sodium -- Water Reactions in LMFBR Steam Generators", Paper E4/5*, 3rd SMiRT, London, September 1975.

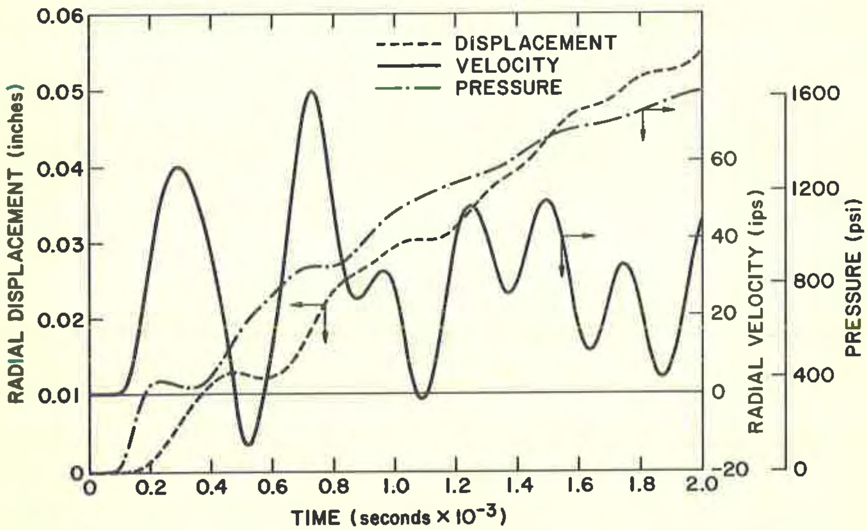

Fig. 1: Pressure, Radial Displacement, and Radial Velocity Histories at Shell Mid-Span.

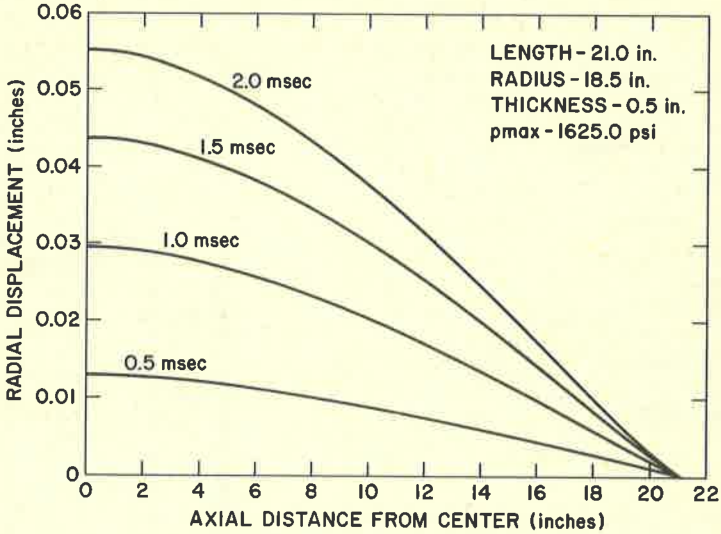

Fig. 2: Radial Displacement Profiles at Selected Times.

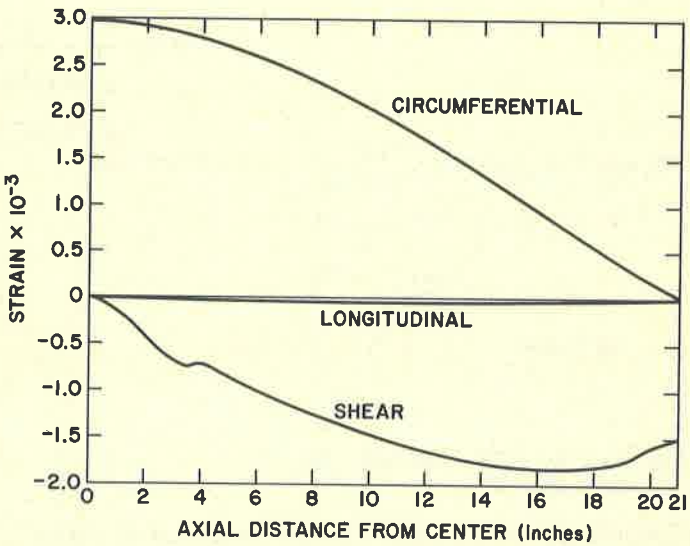

Fig. 3: Strain Profiles at t = 2msec.

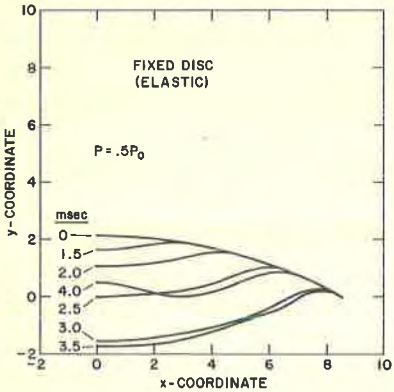

Fig. 4:
Rupture Disk Displacement Profiles at Selected Times.

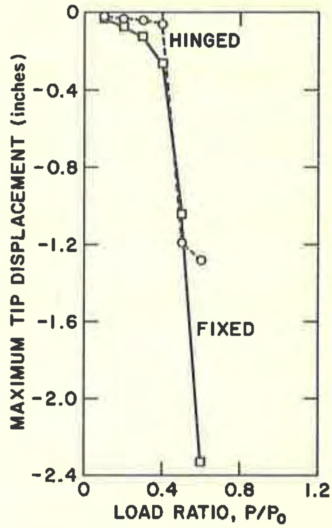

Fig. 6: Equilibrium Path for Fixed and Hinged Disks.

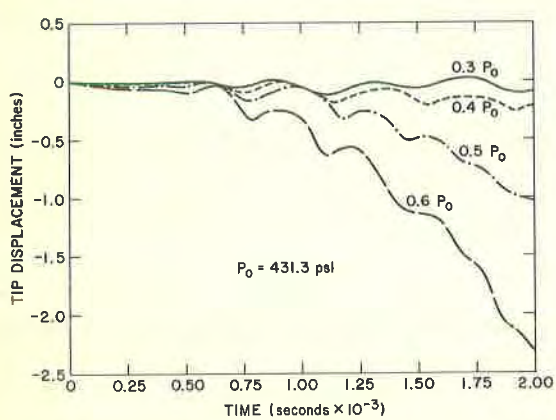

Fig. 5: Disk Apex Displacement Histories at Selected Step Pressure Ratios.